ACS Catalysis

Research Article

pubs.acs.org/acscatalysis

Theoretical Study on the Mechanism of Photoreduction of CO_2 to CH_4 on the Anatase TiO_2(101) Surface

Yongfei Ji[†] and Yi Luo*[,†,‡]

[†]Department of Theoretical Chemistry and Biology, School of Biotechnology, Royal Institute of Technology, SE-106 91 Stockholm, Sweden

[‡]Hefei National Laboratory for Physical Sciences at the Microscale, University of Science and Technology of China, Anhui 230026, People's Republic of China

Supporting Information

ABSTRACT: Artificial photosynthesis of CO_2 has recently attracted intense attention as a potential solution for the energy crisis and global warming. However, the molecular mechanism of the reaction is quite complicated and is far from understood. We performed a first-principles calculation on the thermodynamically feasible formaldehyde pathway: $CO_2 \rightarrow HCOOH \rightarrow H_2CO \rightarrow CH_3OH \rightarrow CH_4$. The interconversion of the C1 molecules has been systematically investigated. We find that a two-electron process has a lower barrier than a one-electron process for the photoreduction of all of the molecules under investigation except for methanol. On the basis of the full potential energy surface for photoreduction of CO_2 to methane, the rate-limiting step is found to be the photoreduction of formic acid to formaldehyde, which contains the elementary step that has the largest kinetic barrier. It will be more efficient if CO instead of formic acid is the precursor of formaldehyde. Then the rate-limiting step becomes the photoreduction of CO_2 to CO. However, the barriers for the photoreduction of the organic molecules are all higher than the barriers for their photodecomposition reaction, which suggests that all of the C1 organic molecules are more easily oxidized than reduced. Thus, charge separation is crucial for improving the efficiency and selectivity of the reaction. The intertwining of photoreduction and photooxidation reactions might be one of the major reasons for the complexity and low efficiency of the reaction. On the basis of the calculations, a new mechanism for the reaction is proposed.

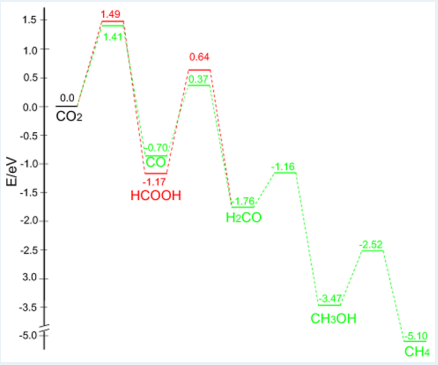

KEYWORDS: *artificial photosynthesis, TiO_2, solar energy, density functional theory, potential energy surface*

1. INTRODUCTION

Photoreduction of CO_2 has attracted great attention recently because it is a potential solution for both the energy crisis and global warming simultaneously.[1−6] Photoreduction of CO_2 into organic molecules using TiO_2 and other semiconductors was first achieved by Inoue et al. in 1979.[7] The work has inspired many continuing studies. Methane (CH_4), methanol (CH_3OH), CO, formic acid (HCOOH), and formaldehyde (H_2CO) are generally formed as products. However, the detailed product distribution was found to depend a great deal on the experimental conditions: the preparation of the catalyst[5] (defects, crystal faces, doping, ...), reaction conditions[8] (temperature, pH, CO_2 concentration, ...), the cocatalyst,[9] and so on. A detailed mechanism of the reaction is far from understood, not to mention control of the selectivity.

The overall photoreduction reaction of CO_2 to CH_4 is a very complicated process which includes the transfer of eight electrons and eight protons, breaking of C−O bonds, and formation of C−H bonds. One simple way to understand the mechanism is to assume that there are two alternative pathways.[2,3,5] One is called the formaldehyde pathway or fast hydrogenation pathway, in which the reaction follows the path $CO_2 \rightarrow HCOOH \rightarrow H_2CO \rightarrow CH_3OH \rightarrow CH_4$. This pathway is thermodynamically feasible, and all the intermediates have been found in various experiments. However, CH_3OH appears as an intermediate, not the final product, and the kinetic model based on this mechanism cannot explain the concentration profile of the product observed in the experiment.[10] The other alternative is the carbene pathway (the fast deoxygenation pathway), in which CO_2 is reduced along the path $CO_2 \rightarrow CO \rightarrow C^{\bullet} \rightarrow CH_3^{\bullet} \rightarrow CH_3OH/CH_4$. The intermediate radicals $C^{\bullet}$ and $CH_3^{\bullet}$ have been detected by EPR experiments,[11,12] and the product profile of many experiments can be fitted to the kinetic model on the basis of this mechanism.[10,13] However, formation of HCOOH and H_2CO are apparently not included in this pathway. It is possible that the reaction can proceed via both routes and the final product depends on which route is the dominating one. Viewing the reaction in this way might be convenient, but none of the pathway has been verified experimentally. More efforts, especially theoretical calculations, are needed to unravel the molecular mechanism of this multistep reaction.

Received: November 27, 2015
Revised: February 8, 2016
Published: February 12, 2016

DOI: 10.1021/acscatal.5b02694
ACS Catal. 2016, 6, 2018−2025

Although the formaldehyde pathway has many problems, it is thermodynamically feasible.[1,2] In addition, it is also important to investigate the interconversion between the C1 molecules to understand the selectivity of the product. Thus, we performed a first-principles calculation on this pathway on the anatase $TiO_2(101)$ surface. This pathway contains two hydrogenation steps ($CO_2 \rightarrow HCOOH$, $H_2CO \rightarrow CH_3OH$) and two deoxygenation steps ($HCOOH \rightarrow H_2CO$, $CH_3OH \rightarrow CH_4$). Each step on the pathway contains the transfer of two electrons and two protons, which largely simplified the overall reaction because it excludes the multielectron and multiproton transfer reactions. However, there are still many possible reactions that need to be considered at each step because, in principle, the electrons can transfer before or after or concerted with one or two protons, and two electrons may also be transferred at a single step. As shown in Scheme 1, in the hydrogenation step,

Scheme 1. Possible Reactions Involved in the Hydrogenation Steps[a]

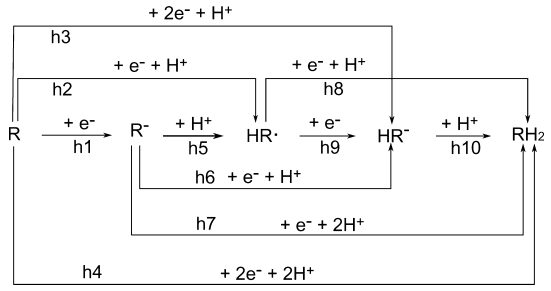

[a]R could be CO_2, CO, or H_2CO.

at least 10 reactions may be involved. Fortunately, many processes, such as reaction 1 in Scheme 1, have very high redox potentials (1.9 eV for R = CO_2) and can be ruled out in calculations. Proton-coupled electron transfer is usually energetically more favorable. In fact, photoreduction of CO_2 to HCOOH has been studied by both experiments[12] and theoretical calculations.[14] It was proposed that CO_2 is most efficiently reduced via the two-electron path, which includes reactions h3 and h10 in Scheme 1. Out of similar considerations and information from experiments, only the reasonable reactions are investigated for each hydrogenation step in the formaldehyde pathway. Usually, we consider the one-electron pathway which includes reactions h2 and h8 (or h2, h9, and h10), and the two-electron pathway, which includes reactions h3 and h10. In reaction h4, two electrons and two protons are transferred in a single step of the reaction. This might be difficult because not enough electrons and protons might be available under real reaction conditions; on the other hand, it is reasonable to assume the existence of intermediates for such a complicated reaction. Therefore, reaction h4 is also not considered in our calculations.

Deoxygenation reaction steps in the formaldehyde pathway are much more complicated because the pathway involves not only the formation of new C−H and/or O−H bonds but also the breaking of a C−OH bond. More reactions than the hydrogenation steps need to be considered. For example, after the transfer of one electron, the possible products could be R$^\bullet$ and hydroxyl anion (OH^-) (reaction d1), or R^- and hydroxyl radical ($^\bullet$OH) (reaction d2) after the breaking of the C−OH bond, which increases the number of reactions that need to be considered. We will not consider reactions such as reaction d3 because we cannot locate that kind of local minimum. Reaction d6″ will also not be studied, because it involves the formation and/or breaking of too many bonds, which requires a large change in the structure of the reactants. However, little information is available to further reduce the number of possible routes. In our calculations, we will first calculate the reaction energies of reactions of interest to determine whether it is necessary to calculate their transition states. This method turns out to be quite efficient, because many reactions in Scheme 2 are quite endothermic. Reactions such as direct

Scheme 2. Possible Reactions Involved in the Deoxygenation Steps[a]

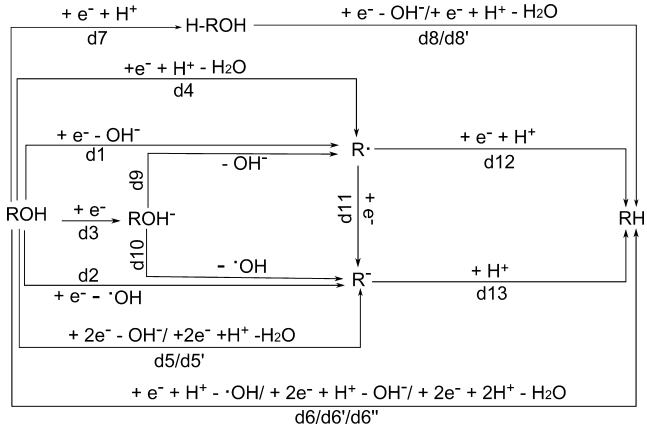

[a]R could be HCO or CH_3.

dissociation of ROH into the two radicals R$^\bullet$ and $^\bullet$OH (highly endothermic) are even not included in Scheme 2. Only transition states of a few reactions need to be calculated.

In each step of the reaction, the pathway in which electrons are transferred one by one is called the one-electron path, and the pathway in which two electrons are transferred in a single elementary step is called the two-electron path. After the calculation of the potential energy surfaces (PES) of each step in the formaldehyde pathway, we will obtain the full PES of the overall reaction, which allows us to find the rate-limiting step. In combination with our previous study[15] on the photooxidation of the C1 organic molecules, the mechanism of the overall reduction reaction of CO_2 will be discussed, and a possible mechanism which is compatible with the formaldehyde and the carbene pathway for the CO_2 photoreduction is proposed in this work.

2. COMPUTATIONAL METHODS

The theoretical method we used to study the photoreduction of CO_2 is similar to that applied in our previous work for the photooxidation of small organic molecules on the anatase $TiO_2(101)$ surface.[15] All calculations were performed with the density functional theory (DFT) implemented in VASP.[16−20] The PBE[21] functional and the PAW[22] pseudopotential have been adopted. The anatase $TiO_2(101)$ surface was presented by a five-layer slab with the center layer fixed and both sides fixed. This avoids the artificial localization of holes at the fixed side of the slab (if one side of the slab is fixed) and stabilizes the radicals in the photocatalytic reactions. This slab model has been applied successfully in our previous studies on the mechanisms of several photoreactions.[15,23−26] In our calculation, a 3 × 1 supercell along the [010] and [10$\bar{1}$] directions

DOI: 10.1021/acscatal.5b02694
ACS Catal. 2016, 6, 2018−2025

with a vacuum layer of 13 Å has been used. The slab contains 180 atoms, and all calculations were performed at the Γ point. The structures were relaxed until the maximum force on the atoms was smaller than 0.02 eV/Å. The transition states were searched with the nudged elastic band method with climbing images.[27]

H atoms were adsorbed on the surface to supply conduction band electrons and protons for the photoreduction of the molecules. In artificial photosynthesis, water is suggested to be oxidized by the photogenerated hole to O_2 and protons;[12,28] then the protons and the photogenerated electrons are used to reduce CO_2. In theoretical calculations, it is equivalent to use adsorbed H atoms to study the reduction of the molecules. The solution effect was neglected because of the difficulty in the theoretical description of the liquid/solid interface. The same method has been applied by He et al.[14] It is worth mentioning that part of the photogenerated charge carriers (electrons and holes) will undergo trapping before they transfer to adsorbates.[29] Modeling of the trapped charge carriers requires higher level methods such as using hybrid functionals[30] to overcome the self-interaction error[31] in DFT. However, this kind of calculation is extremely expensive. An alternative way is to use the GGA+U[25,32] method, which only increases the computation effort slightly. However, the results usually depend on the *U* value. As a compromise, we performed single-point calculations with the HSE hybrid functional[33] on the GGA+U optimized structures (GGA+U/HSE). A test calculation with a small TiO_2 model shows that this gives results very close to those of pure HSE calculations. Therefore, the GGA+U/HSE method has been used for the calculation on the large supercell used in this work. A comparison of the results from these three methods (GGA+U, GGA+U/HSE, HSE) on the small TiO_2 model and a comparison of results on the large supercell with the GGA, GGA+U, and GGA+U/HSE methods can be found in the Supporting Information. Although the GGA and GGA +U calculations agree with the GGA+U/HSE method qualitatively, they might give the wrong rate-limiting step of the overall reaction.

3. RESULTS AND DISCUSSION

3.1. Photoreduction of CO_2 to HCOOH and CO. Photoreduction of CO_2 to HCOOH and CO (reactions 1 and 2) have been theoretically studied by He et al.[14] They considered the one-electron path, which includes reactions h1, h6, and h10, and the two-electron path, which includes reactions h3 and h10, for the photoreduction of CO_2 to HCOOH. The two-electron pathway was found to have a lower barrier. In reaction h3, two electrons are transferred concertedly with a proton to the linear CO_2 (state A1), forming a monodentate formate (state B1) which recombines with a proton nearly barrierlessly to form a HCOOH molecule (state C1 in Figure 1a). In our calculations, the second step (reaction h10) is also nearly barrierless. However, the barrier for reaction h3 is calculated to be 1.49 eV, which is much larger (and the released heat is much smaller) than that reported by He et al.[14] Part of the reason for this difference must come from the difference in the computational details. We notice that a quite small supercell has been used in their work: a 2 × 1 three-layer slab. The relative energies (in eV) of the initial, intermediate, and final states (A1, B1, and C1 in Figure 1a) in our GGA calculation are 0.00, −0.24, and −0.76. When we use the same supercell as theirs, the relative energies become 0.00, −0.80, and −1.29, which are much closer to their results (0.00, −1.12, −1.68). This suggests that the supercell in their work is too small and the barriers for the photoreduction of CO_2 might have been underestimated.

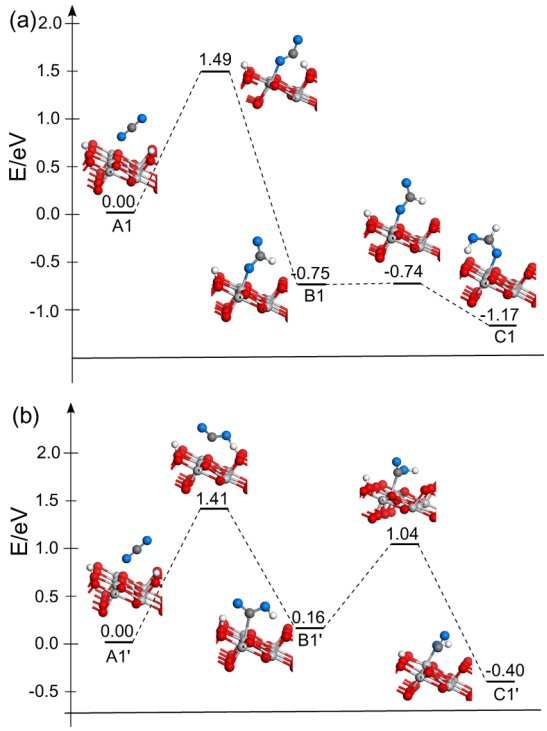

Figure 1. Potential energy surfaces for the photoreduction of CO_2: (a) photoreduction of CO_2 to HCOOH; (b) photoreduction of CO_2 to CO. Blue, red, gray, and dark gray atoms depict oxygen atoms from the molecule, oxygen atoms of TiO_2, and Ti and C atoms, respectively.

$$CO_2 + 2H^+ + 2e^- \rightarrow HCOOH \quad (1)$$

$$CO_2 + 2H^+ + 2e^- \rightarrow CO + H_2O \quad (2)$$

Photoreduction of CO_2 to CO (reaction 2) was also investigated. We still chose the linear CO_2 as the initial state (A1′ in Figure 1b) because it is the most stable configuration of the molecule.[14,34] $COOH^-$ is located as the intermediate state (B1′ in Figure 1b) with a barrier of 1.41 eV from state A1′. This species has also been proposed to be the intermediate in the electrochemical reduction of CO_2.[35] The intermediate state is quite similar to that in the previous work by He et al.;[14] it decomposes to CO and OH^- with a barrier of 0.88 eV, which results in a total barrier of 1.41 eV. This suggests that it is a little easier for CO_2 to be reduced to CO. In some experiments, CO was found to be the major product.[36,37] It was suggested that the surface defects play important roles in these experiments. CO_2 at the oxygen vacancy can even dissociate spontaneously at room temperature.[34,37] Thus, CO can be easily produced and may be further photoreduced to organic molecules.

3.2. Photoreduction of HCOOH to H_2CO. Reduction of HCOOH to H_2CO is a deoxygenation reaction (reaction 3). Direct transfer of one electron is very difficult (reaction d3 for R = HCO); we see no noticeable increase of the negative charge on the molecule in the presence of excess electrons on TiO_2. We also find that direct hydrogenation (reaction d7) of the oxygen atom in the HCOOH molecule is also not possible. It will just decompose back to the HCOOH. Therefore, reactions d3 and d7 cannot happen, which suggests that the

DOI: 10.1021/acscatal.5b02694
ACS Catal. 2016, 6, 2018−2025

electron transfer must be coupled with the breaking of the R−OH bond. The product could be a formyl radical ($HCO^{\bullet}$) with OH^- (reaction d1), or a $^{\bullet}OH$ radical with a formyl anion (HCO^-) (reaction d2) if the electron transfer is not coupled with the proton transfer concertedly; otherwise, the product should be a H_2CO molecule with a $^{\bullet}OH$ radical (reaction d6) or a H_2O molecule with a $HCO^{\bullet}$ radical (reaction d4). In recent experiments,[38] reaction d1 was suggested to happen. It was proposed that the product could be stabilized if the OH^- anion was adsorbed to an nearby Ti atom. Although the product is stable in our calculations, the reaction was found to be highly endothermic by 1.68 eV (state C2 in Figure 2).[38] This

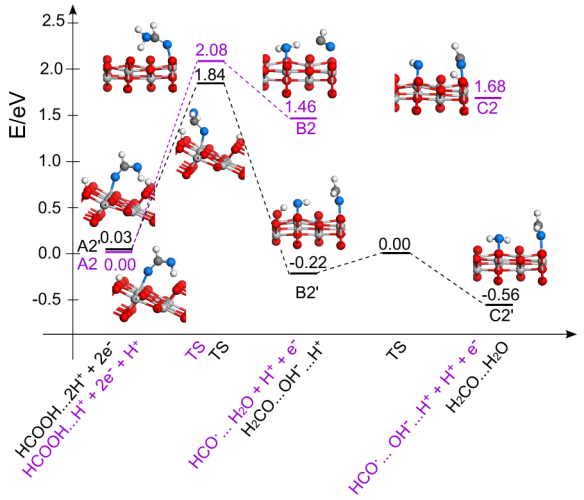

Figure 2. Potential energy surface for the photoreduction of HCOOH. One electron is transferred in the purple path and two electrons at the first step of the black path. M···H^+ indicates that H^+ is adsorbed near M and M + H^+ indicates that H^+ is adsorbed far from M.

can be rationalized by noticing that the overall reaction (reaction 3) is only slightly exothermic,[1] whereas the recombinations of the OH^- anion with proton to give H_2O and that of $HCO^{\bullet}$ with H to give H_2CO are both highly exothermic.[15] We failed to get the product in reaction d2, which suggests that it is less stable than the product in reaction d1. In the concerted pathway, we find that reaction d4 has the lowest reaction energy of 1.46 eV (reaction d6 is more endothermic than reaction d1 because oxidation of HCOH is exothermic[15]). Thus, we will just calculate the PES of reaction d4 (state A2 to B2 in Figure 2). As shown in Figure 2, the proton attacks the O atom in the HCOOH molecule, forming a H_2O molecule and a $HCO^{\bullet}$ radical. The barrier is calculated to be as high as 2.08 eV. The $HCO^{\bullet}$ can recombine with a nearby proton to form H_2CO (reaction d15) easily. A more detailed discussion about this reaction will be provided in the next section.

$$HCOOH + 2e^- + 2H^+ \rightarrow H_2CO + H_2O \quad (3)$$

Then we consider the two-electron path (Figure 2). To align the energies of the two reaction paths, we assume that, in the one-electron path, another H atom is adsorbed far away from the molecule.[14] When the H atom comes near the molecule, the energy of the system is calculated to be increased by 0.03 eV. There are also four possible reactions that might be the first step of the two-electron path: reactions d5, d5′ d6′, and d6″. In reaction d5, HCOOH is directly dissociated into HCO^- and OH^- and the reaction is highly endothermic by 0.84 eV; in reaction d5′ one proton is transferred concertedly to form H_2O, which lowers the reaction energy to 0.51 eV. However, reaction d5′ is quite similar to reaction d4, which may have a high barrier. The difference between d5 (d5′) and d6′ (d6″) is that one more proton is transferred in the latter reaction. Reaction d6′ is exothermic by 0.22 eV and reaction d6″ by 0.56 eV. Reaction d6″ will not be considered as mentioned in the Introduction. Thus, we chose to calculate the PES of reaction d6′ (state A2′ to B2′ in Figure 2). As shown in Figure 2, the proton now attacks the C atom in the HCOOH molecule. The calculated barrier for this reaction is much lower than that for reaction d4 but is still as high as 1.81 eV. Further recombination of the OH^- with a proton to form H_2O (state B2′ to C2′) has a smaller barrier of 0.22 eV. Thus, the total barrier is 1.81 eV, which is much higher than the calculated barrier for the reduction of CO_2 to HCOOH.[14] Therefore, this step might be the rate-limiting step for the photoreduction of CO_2 to CH_3OH and/or CH_4. Other pathways for the formation of H_2CO such as hydrogenation of CO might need to be considered.

3.3. Photoreduction of CO to H_2CO. For the hydrogenation of CO to H_2CO (reaction 4), we failed to obtain species such as CO^- or HCO^+ ion adsorbed on the surface, which means that the electron transfer must be coupled with the proton transfer concertedly (reaction h2 for R = CO in Scheme 1). As shown in Figure 3, the reaction is endothermic

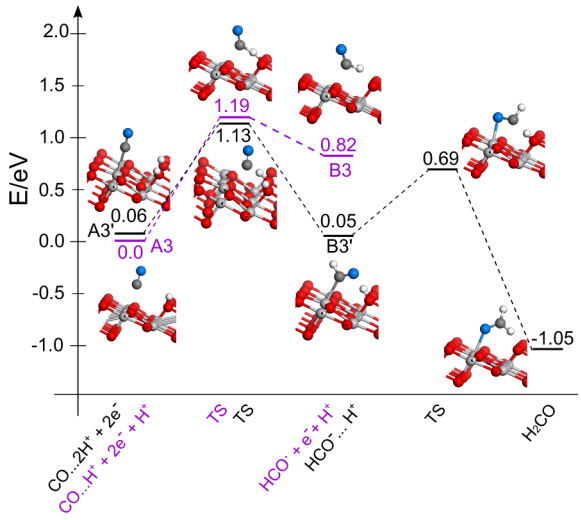

Figure 3. Potential energy surfaces for the photoreduction of CO. One electron is transferred in the purple path, and two electrons are transferred at the first step of the black path.

by 0.82 eV with a barrier of 1.19 eV (state A3 to B3). Then we come to the reduction reaction of $HCO^{\bullet}$ to H_2CO again. In principle, the reaction can be a concerted process (reaction h8) or a stepwise process which includes reactions h9 and h10. To study reaction h8, we have to put the system in the singlet state. However, when we do this, the electron will transfer to the $HR^{\bullet}$ radical and form HR^- spontaneously. This process corresponds to reaction h9, and then we only need to deal with reaction h10. However, for $HCO^{\bullet}$, when we placed a H to the nearest bridge oxygen to $HCO^{\bullet}$ in state B3, we found that it will recombine with the proton to H_2CO barrierlessly at the singlet state, which is consistent with our previous study.[15] We also succeeded in obtaining the structure of adsorbed HCO^- by rotating the molecule to point the C−O bond to the H atom

DOI: 10.1021/acscatal.5b02694
ACS Catal. 2016, 6, 2018−2025

(state B3′ in Figure 3). The barrier for the recombination of HCO^- with proton to give H_2CO was calculated to be 0.64 eV. Therefore, the barrier in the one-electron path is 1.19 eV.

$$CO + 2H^+ + 2e^- \rightarrow H_2CO \quad (4)$$

In the two-electron path, HCO^- will form after one proton transfers concertedly with two electrons to CO (reaction h3, state A3′ to B3′ in Figure 3). As shown in Figure 3, this reaction has a barrier of 1.07 eV, which is slightly lower than that for the one-electron path. The calculation is spin-unrestricted, and we found that the transition state is neither in the singlet nor in the triplet state. The magnetic moment at the HCO group in the transition state is 0.33 μ_B, which is slightly larger than that in the transition state in the one-electron path (0.30 μ_B). This suggests that slightly more charge is transferred to CO in the two-electron path, which results in a slightly lower barrier. Considering that the barrier for the reduction of HCOOH to H_2CO is 1.81 eV, hydrogenation of CO is more efficient.

3.4. Photoreduction of H_2CO to CH_3OH. The next step in the formaldehyde pathway is the hydrogenation of H_2CO to give CH_3OH (reaction 5). As in the hydrogenation of CO, we calculated reactions h2, h9, and h10 in the one-electron path: H_2CO is first reduced to methoxyl radical ($CH_3O^•$) (reaction h2), which then captures an electron to form methoxyl anion (CH_3O^-) (reaction h9), and this recombines with a proton to form CH_3OH (reaction h10). As shown in Figure 4, the

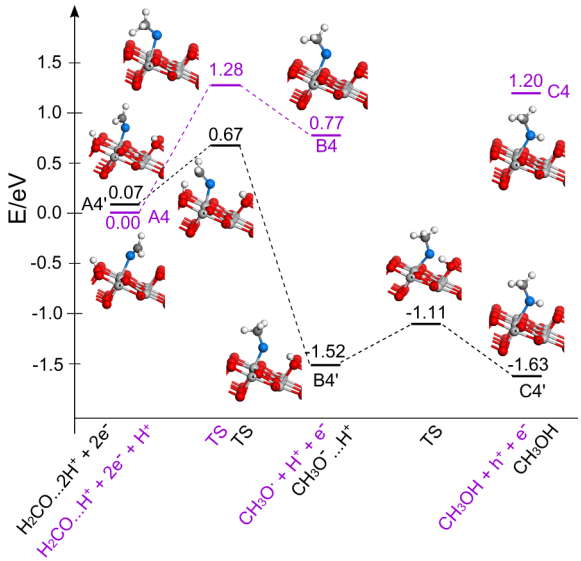

Figure 4. Potential energy surfaces for the photoreduction of H_2CO. One electron is transferred at the first step of the purple path, and two electrons are transferred at the first step of the black path.

photoreduction of H_2CO to $CH_3O^•$ (state A4 to B4) is endothermic by 0.77 eV with a barrier of 1.28 eV. According to our previous work,[15] $CH_3O^•$ can recombine with a proton to form CH_3OH at the triplet potential energy surface (state B4 to C4). In this pathway, $CH_3O^•$ is not reduced by a conduction band electron but a valence band electron, and the reaction is endothermic by 0.43 eV. Only when the system goes from the triplet state to the singlet state (C4 to C4′) will the photoreduction reaction be completed. The reverse process (C4′ → C4 → B4 → A4) is the stepwise photodecomposition of CH_3OH to H_2CO, which has been observed in a recent experiment.[39] For the photoreduction of H_2CO to CH_3OH, it does not necessarily follow this pathway back. Via reaction h9, $CH_3O^•$ in the intermediate state B4 can capture a conduction band electron and turns into CH_3O^- (state B4′); then via reaction 10, CH_3O^- will combine with a proton to form CH_3OH (state C4′) by overcoming a smaller barrier of 0.41 eV. The rate-limiting step in this pathway (A4 → B4 → B4′ → C4′) is the first step, which has a barrier of 1.28 eV. This is much more efficient than the reverse reaction of photodecomposition of CH_3OH.

$$H_2CO + 2H^+ + 2e^- \rightarrow CH_3OH \quad (5)$$

In the two-electron path, H_2CO is assumed to be reduced to CH_3O^- directly after the transfer of two electrons and one proton to H_2CO (reaction h3). As shown in Figure 4, the barrier of this reaction (A4′ to B4′) is 0.60 eV, which is much smaller than that in the one-electron pathway (A4 to B4). This is consistent with a recent experiment which suggested that H_2CO can only be reduced in a two-electron process or just serves as a hole scavenger.[40] The two-electron photoreduction is highly exothermic by 1.59 eV, which results in a barrier of 2.19 eV for its reverse reaction (B4′ to A4′). This explains why CH_3O^- is thermally stable but can be easily photodecomposed.[39]

3.5. Photoreduction of CH_3OH to CH_4. Reduction of CH_3OH to CH_4 is again a deoxygenation reaction (reaction 6). Four reactions may happen as the first step of the one-electron path: reactions d1, d2, d4, and d6. In reactions d1 and d2, the molecule decomposes after the attachment of the electron. We can only obtain the product in reaction d1, in which CH_3OH is decomposed into $CH_3^•$ and OH^- (state A5 to B5 in Figure 5). The reaction is endothermic by 0.67 eV with a barrier of 0.95 eV. At the transition state, we can see that the C−O bond in the molecule breaks and a planar $CH_3^•$ radical is formed. The OH^- then recombines with a proton to form a H_2O molecule (B5 to C5). In this process (A5 → B5 → C5), the electron and the proton transfer in a stepwise way. In the concerted pathway,

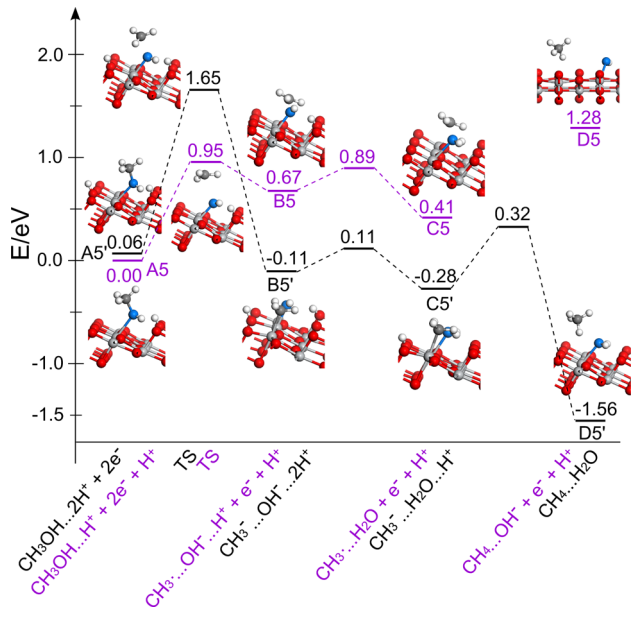

Figure 5. Potential energy surfaces for the photoreduction of CH_3OH. One electron is transferred at the first step of the purple path, and two electrons are transferred at the first step of the black path.

DOI: 10.1021/acscatal.5b02694
ACS Catal. 2016, 6, 2018−2025

the proton recombines either with the methyl to form a CH_4 or with the hydroxyl to form a H_2O. In the former case (reaction d6), the reaction energy is 1.28 eV (state D5), which is already higher than the barrier of the stepwise pathway. In the latter case (reaction d4), the same transition state with the stepwise pathway was located. Different from the photoreduction of other molecules above, CH_3OH seems to favor the stepwise pathway rather than the concerted path. $CH_3^•$ formed in reaction d1 then turns into a methyl anion (CH_3^-) by capturing a conduction band electron (C5 to C5′). The recombination of the CH_3^- with a proton (C5′ to D5′) is exothermic by 1.28 eV with a barrier of 0.60 eV. Thus, the rate-limiting step for the one-electron pathway (A5 → B5 → C5 → C5′ → D5′) is the first step to form $CH_3^•$.

$$CH_3OH + 2H^+ + 2e^- \rightarrow CH_4 + H_2O \quad (6)$$

In the two-electron pathway, there are also four possible reactions as the first step: reactions d5, d5′, d6′, and d6″ (not considered). In reaction d5, CH_3OH is decomposed to $HCO^•$ and OH^- (state A5′ to B5′ in Figure 5). The calculated barrier is 1.59 eV, which is larger than that for the one-electron pathway. This is also different from other molecules investigated in this work, which all have a lower barrier in the two-electron pathway. The calculation is spin unrestricted; we found that the transition state is in the triplet state, and we can still see the formation of a planar $CH_3^•$. This suggests that the transition state is essentially the same as that in the one-electron pathway. Therefore, we are not going to investigate the concerted pathway in which the proton is transferred concertedly to form H_2O (reaction d5′, state A5′ to C5′ in Figure 5) because the same transition state with reaction d5 should be located as in the one-electron path. In reaction d6′, the proton attacks the carbon to form a CH_4 molecule directly. The barrier for this reaction is calculated to be as high as 3.94 eV (GGA result, structure not shown in Figure 5).

Thus, the most efficient pathway in the two-electron reaction is via reaction d5. The slightly higher barrier in comparison to the one-electron pathway may come from the additional repulsion between the $CH_3^•$ and another H atom and the activation of the other localized electron for its transfer. The rest of the reaction is the recombination of OH^- and CH_3^- with a proton to form H_2O and CH_4. It does not matter which happens first, the rate-limiting step is still the breaking of the C−O bond in CH_3OH.

Although $CH_3^•$ was detected by EPR experiments[12] in the photoreduction of CO_2, it is missing in the photocatalytic reaction of CH_3OH.[40] This suggests that $CH_3^•$ cannot come from one-electron reduction of CH_3OH. However, our calculations show that the barrier of the one-electron reduction of CH_3OH is lower than the reduction of CO_2 to CO and the reduction of H_2CO to CH_3OH. Thus, it is kinetically feasible for this one-electron process to happen. It is possible that CH_3OH is only readily oxidized in the setup of that experiment.[40]

3.6. Mechanism of Photoreduction of CO_2. On the basis of the calculations above, we can now plot the full potential energy surface for the reaction. In Figure 6, we only show the effective barrier for the interconversion between the C1 molecules. Bear in mind that the reaction energy for the photoreduction of CO_2 to CO is −0.70 eV; it is −0.40 eV in Figure 1b because we did not take into account the released heat for the recombination of OH^- with H^+ to give H_2O.[15] Now we have two reaction paths: path I, CO_2 → HCOOH → H_2CO → CH_3OH → CH_4; path II, CO_2 → CO → H_2CO → CH_3OH → CH_4. In path I, the rate-limiting step is the photoreduction of HCOOH to H_2CO, which contains an elementary step with a barrier of 1.81 eV. This is much larger than the barrier for the photoreduction of CO_2 to CO (1.41 eV). In path II, photoreduction of CO_2 to CO now becomes the rate-determining step. These suggests that deoxygenation of the molecules on the ideal surface is very difficult. On the other hand, all of the organic molecules have a lower barrier for the photooxidation reaction than for the photoreduction reaction.[15] This means that it is easier for the molecules to be photooxidized than to be photoreduced, which implies that charge separation is essential for the photoreduction of CO_2. The intertwining of the photooxidation reaction and the photoreduction reaction may be one of the major reasons for the low efficiency and complexity of the CO_2 photoreduction reaction. Among the organic molecules, H_2CO has the lowest barrier in the photooxidation reaction[15] and photoreduction reaction; this explains why it is usually not found in the experiments. In some experiments, HCOOH was also found as the major product. Usually such experiments used liquid[41] CO_2 or supercritical[42] CO_2; the reaction equilibrium between CO_2 and HCOOH may forbid the HCOOH to be photooxidized back to CO_2. On the other hand, the barrier of photoreduction of HCOOH to H_2CO is also very high, which is possibly why HCOOH can survive as the final product.

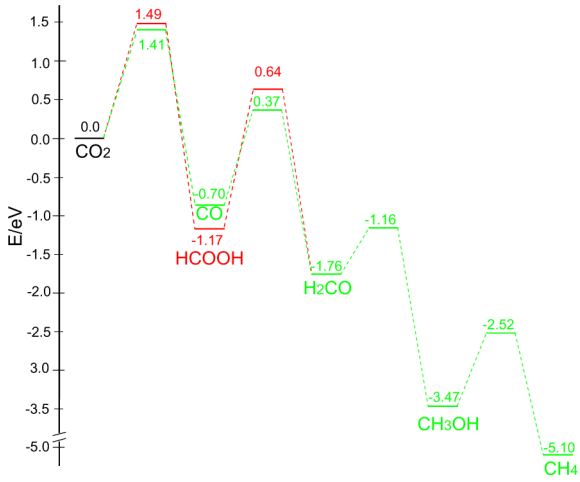

Figure 6. Full potential energy surfaces for the photoreduction of CO_2 to CH_4.

As we mentioned before, the formaldehyde pathway is not consistent with some experiments. Our calculation proposed a new pathway which involves CO in it (path II). However, it still suffers from the same problem as the formaldehyde pathway, in that it cannot explain the product profile observed in some experiments. Our calculations have been done on the ideal anatase TiO_2(101) surface. A recent study has shown that surface defects,[36] such as oxygen vacancy (O_v), play an important role because they can make the deoxygenation process easier. CO_2 adsorbed in the oxygen O_v can easily dissociate to form CO.[34,37] It may have a similar effect for the activation of CO. H_2CO and CH_3OH formed via the hydrogenation of CO adsorbed at O_v cannot escape due to the strong adsorption of the molecules at O_v. However, $CH_3^•$, which can recombine with OH to form CH_3OH or H to form CH_4, can form via the breaking of the C−O bond (after CO is hydrogenated to CH_3O at O_v) because deoxygenation is easier

DOI: 10.1021/acscatal.5b02694
ACS Catal. 2016, 6, 2018−2025

at O_v. Such a pathway is similar to path II happening at O_v except for the final step. Bear in mind that CO adsorbed at an oxygen vacancy is stoichiometrically equivalent to C adsorbed on an ideal TiO_2 surface. Therefore, it is essentially quite similar to the carbene pathway. The kinetic model based on this path should also fit the product profile observed in the experiments.[10,13]

Thus, we propose a new mechanism for the photoreduction of CO_2 to CH_4: on an ideal surface, it follows the path $CO_2 \rightarrow CO \rightarrow H_2CO \rightarrow CH_3OH \rightarrow CH_4$; at O_v this path is modified to $CO_2 \rightarrow CO \rightarrow H_2CO \rightarrow CH_3^{\bullet} \rightarrow CH_4/CH_3OH$, which is similar to the carbene pathway. However, one has to remember that photoreduction of CO_2 to CH_4 is a multistep reaction which involves the transfer of eight electrons and eight protons, breaking of two C−O bonds, and formation of four C−H bonds. Too many aspects need to be considered to fully understand the overall reaction. For example, the existence of surface species such as hydroxyl groups might affect the formation of carbonate-like species,[12] which adds up to the complexity of the reaction. There is a great deal of room for other reaction routes, which are out of the scope of the current study.[38,43]

4. CONCLUSION

In conclusion, we have carried out a systematic theoretical study on the photoreduction of CO_2 to CH_4. For the reduction of the C1 molecules, the two-electron path usually has a lower barrier than the one-electron path except for CH_3OH. However, for all the organic molecules, the barriers for the photooxidation of molecules are lower than those for their photoreduction reactions. Thus, charge separation is important to improve the efficiency and selectivity of the reaction. In the formaldehyde pathway, a high barrier for the photoreduction of HCOOH to H_2CO was found. It is more efficient for the CO_2 to be photoreduced to H_2CO via the intermediate CO. In this new pathway, the rate-determining step becomes the photoreduction of CO_2 to CO. These suggests that an oxygen vacancy can be a more active site for the reaction because deoxygenation becomes easier at it. A new mechanism which is compatible with the formaldehyde and the carbene pathway is proposed.

■ ASSOCIATED CONTENT

Supporting Information

The Supporting Information is available free of charge on the ACS Publications website at DOI: 10.1021/acscatal.5b02694.

Test calculationd on a small TiO_2 model and GGA and GGA+U results of the potential energy surface on the large TiO_2 model (PDF)

■ AUTHOR INFORMATION

Corresponding Author

*E-mail for Y.L.: luo@kth.se.

Notes

The authors declare no competing financial interest.

■ ACKNOWLEDGMENTS

This work was supported by the NBRP (grants 2010CB923300 and 2011CB921400) of China, the Göran Gustafsson Foundation for Research in Natural Sciences and Medicine, the Swedish Research Council (VR), the National Natural Science Foundation of China (21421063), and the Strategic Priority Research Program of the Chinese Academy of Sciences (XDB01020200). The Swedish National Infrastructure for Computing (SNIC) is acknowledged for computer time.

■ REFERENCES

(1) Mao, J.; Li, K.; Peng, T. Y. *Catal. Sci. Technol.* **2013**, *3*, 2481−2498.
(2) Habisreutinger, S. N.; Schmidt-Mende, L.; Stolarczyk, J. K. *Angew. Chem., Int. Ed.* **2013**, *52*, 7372−7408.
(3) Dhakshinamoorthy, A.; Navalon, S.; Corma, A.; Garcia, H. *Energy Environ. Sci.* **2012**, *5*, 9217−9233.
(4) Kondratenko, E. V.; Mul, G.; Baltrusaitis, J.; Larrazabal, G. O.; Perez-Ramirez, J. *Energy Environ. Sci.* **2013**, *6*, 3112−3135.
(5) Liu, L.; Li, Y. *Aerosol Air Qual. Res.* **2014**, *14*, 453−469.
(6) Izumi, Y. *Coord. Chem. Rev.* **2013**, *257*, 171−186.
(7) Inoue, T.; Fujishima, A.; Konishi, S.; Honda, K. *Nature* **1979**, *277*, 637−638.
(8) Koci, K.; Obalova, L.; Lacny, Z. *Chem. Pap.* **2008**, *62*, 1−9.
(9) Jeyalakshmi, V.; Mahalakshmy, R.; Krishnamurthy, K. R.; Viswanathan, B. *Indian J. Chem. Sect. A* **2012**, *51*, 1263−1283.
(10) Koci, K.; Obalova, L.; Solcova, O. *Chem. Process Eng.* **2010**, *31*, 395−407.
(11) Anpo, M.; Yamashita, H.; Ichihashi, Y.; Ehara, S. *J. Electroanal. Chem.* **1995**, *396*, 21−26.
(12) Dimitrijevic, N. M.; Vijayan, B. K.; Poluektov, O. G.; Rajh, T.; Gray, K. A.; He, H.; Zapol, P. *J. Am. Chem. Soc.* **2011**, *133*, 3964−3971.
(13) Tan, S. S.; Zou, L.; Hu, E. *Catal. Today* **2008**, *131*, 125−129.
(14) He, H. Y.; Zapol, P.; Curtiss, L. A. *Energy Environ. Sci.* **2012**, *5*, 6196−6205.
(15) Ji, Y.; Wang, B.; Luo, Y. *J. Phys. Chem. C* **2014**, *118*, 21457−21462.
(16) Kresse, G.; Hafner, J. *Phys. Rev. B: Condens. Matter Mater. Phys.* **1993**, *47*, 558−561.
(17) Kresse, G.; Furthmuller, J. *Comput. Mater. Sci.* **1996**, *6*, 15−50.
(18) Kresse, G.; Furthmuller, J. *Phys. Rev. B: Condens. Matter Mater. Phys.* **1996**, *54*, 11169−11186.
(19) Kresse, G.; Hafner, J. *Phys. Rev. B: Condens. Matter Mater. Phys.* **1994**, *49*, 14251−14269.
(20) Kresse, G.; Joubert, D. *Phys. Rev. B: Condens. Matter Mater. Phys.* **1999**, *59*, 1758−1775.
(21) Perdew, J. P.; Burke, K.; Ernzerhof, M. *Phys. Rev. Lett.* **1996**, *77*, 3865−3868.
(22) Blöchl, P. E. *Phys. Rev. B: Condens. Matter Mater. Phys.* **1994**, *50*, 17953−17979.
(23) Ji, Y.; Luo, Y. *J. Phys. Chem. C* **2014**, *118*, 6359−6364.
(24) Ji, Y.; Wang, B.; Luo, Y. *J. Phys. Chem. C* **2013**, *117*, 956−961.
(25) Ji, Y.; Wang, B.; Luo, Y. *J. Phys. Chem. C* **2012**, *116*, 7863−7866.
(26) Ji, Y.; Wang, B.; Luo, Y. *J. Phys. Chem. C* **2014**, *118*, 1027−1034.
(27) Henkelman, G.; Jonsson, H. *J. Chem. Phys.* **2000**, *113*, 9978−9985.
(28) Uner, D.; Oymak, M. M. *Catal. Today* **2012**, *181*, 82−88.
(29) Tamaki, Y.; Furube, A.; Murai, M.; Hara, K.; Katoh, R.; Tachiya, M. *Phys. Chem. Chem. Phys.* **2007**, *9*, 1453−1460.
(30) Di Valentin, C.; Pacchioni, G.; Selloni, A. *Phys. Rev. Lett.* **2006**, *97*, 166803.
(31) Mori-Sánchez, P.; Cohen, A. J.; Yang, W. *Phys. Rev. Lett.* **2008**, *100*, 146401.
(32) Dudarev, S. L.; Botton, G. A.; Savrasov, S. Y.; Humphreys, C. J.; Sutton, A. P. *Phys. Rev. B: Condens. Matter Mater. Phys.* **1998**, *57*, 1505−1509.
(33) Heyd, J.; Scuseria, G. E.; Ernzerhof, M. *J. Chem. Phys.* **2003**, *118*, 8207−8215.
(34) Sorescu, D. C.; Al-Saidi, W. A.; Jordan, K. D. *J. Chem. Phys.* **2011**, *135*, 124701−124717.
(35) Peterson, A. A.; Nørskov, J. K. *J. Phys. Chem. Lett.* **2012**, *3*, 251−258.

DOI: 10.1021/acscatal.5b02694
ACS Catal. 2016, 6, 2018−2025

(36) Liu, L. J.; Zhao, H. L.; Andino, J. M.; Li, Y. *ACS Catal.* **2012**, *2*, 1817−1828.
(37) Liu, L.; Zhao, C.; Li, Y. *J. Phys. Chem. C* **2012**, *116*, 7904−7912.
(38) Shkrob, I. A.; Dimitrijevic, N. M.; Marin, T. W.; He, H. Y.; Zapol, P. *J. Phys. Chem. C* **2012**, *116*, 9461−9471.
(39) Guo, Q.; Xu, C.; Ren, Z.; Yang, W.; Ma, Z.; Dai, D.; Fan, H.; Minton, T. K.; Yang, X. *J. Am. Chem. Soc.* **2012**, *134*, 13366−13373.
(40) Dimitrijevic, N. M.; Shkrob, I. A.; Gosztola, D. J.; Rajh, T. *J. Phys. Chem. C* **2012**, *116*, 878−885.
(41) Kaneco, S.; Kurimoto, H.; Ohta, K.; Mizuno, T.; Saji, A. *J. Photochem. Photobiol., A* **1997**, *109*, 59−63.
(42) Kaneco, S.; Kurimoto, H.; Shimizu, Y.; Ohta, K.; Mizuno, T. *Energy* **1999**, *24*, 21−30.
(43) Shkrob, I. A.; Marin, T. W.; He, H. Y.; Zapol, P. *J. Phys. Chem. C* **2012**, *116*, 9450−9460.

DOI: 10.1021/acscatal.5b02694
ACS Catal. 2016, 6, 2018−2025